2017

L2(1) and XA Ordering Competition in Hafnium-Based Full-Heusler Alloys Hf(2)VZ (Z = Al, Ga, In, Tl, Si, Ge, Sn, Pb)

Xiaotian Wang
University of Wollongong, Southwest University, xw573@uowmail.edu.au

Zhenxiang Cheng
University of Wollongong, cheng@uow.edu.au

Wenhong Wang
Chinese Academy Of Sciences, wenhong.wang@aphy.iphy.ac.cn

Publication Details

Wang, X., Cheng, Z. & Wang, W. (2017). L2(1) and XA Ordering Competition in Hafnium-Based Full-Heusler Alloys Hf(2)VZ (Z = Al, Ga, In, Tl, Si, Ge, Sn, Pb). Materials, 10 (10), 1200-1-1200-15.

L2(1) and XA Ordering Competition in Hafnium-Based Full-Heusler Alloys Hf(2)VZ (Z = Al, Ga, In, Tl, Si, Ge, Sn, Pb)

Abstract
For theoretical designing of full-Heusler based spintroinc materials, people have long believed in the so-called Site Preference Rule (SPR). Very recently, according to the SPR, there are several studies on XA-type Hafnium-based Heusler alloys X2YZ, i.e., Hf2VAl, Hf2CoZ (Z = Ga, In) and Hf2CrZ (Z = Al, Ga, In). In this work, a series of Hf2-based Heusler alloys, Hf2VZ (Z = Al, Ga, In, Tl, Si, Ge, Sn, Pb), were selected as targets to study the site preferences of their atoms by first-principle calculations. It has been found that all of them are likely to exhibit the L21-type structure instead of the XA one. Furthermore, we reveal that the high values of spin-polarization of XA-type Hf2VZ (Z = Al, Ga, In, Tl, Si, Ge, Sn, Pb) alloys have dropped dramatically when they form the L21-type structure. Also, we prove that the electronic, magnetic, and physics nature of these alloys are quite different, depending on the L21-type or XA-type structures.

Disciplines
Engineering | Physical Sciences and Mathematics

Publication Details
Wang, X., Cheng, Z. & Wang, W. (2017). L2(1) and XA Ordering Competition in Hafnium-Based Full-Heusler Alloys Hf(2)VZ (Z = Al, Ga, In, Tl, Si, Ge, Sn, Pb). Materials, 10 (10), 1200-1-1200-15.

materials

MDPI

Article

$L2_1$ and XA Ordering Competition in Hafnium-Based Full-Heusler Alloys Hf_2VZ (Z = Al, Ga, In, Tl, Si, Ge, Sn, Pb)

Xiaotian Wang [1,2], Zhenxiang Cheng [2,*] and Wenhong Wang [3]

1 School of Physical Science and Technology, Southwest University, Chongqing 400715, China; wangxt45@126.com or xiaotianwang@swu.edu.cn
2 Institute for Superconducting and Electronic Materials, University of Wollongong, Wollongong 2500, Australia
3 Beijing National Laboratory for Condensed Matter Physics, Institute of Physics, Chinese Academy of Sciences, Beijing 100190, China; wenhong.wang@iphy.ac.cn
* Correspondence: cheng@uow.edu.au

Received: 16 September 2017; Accepted: 15 October 2017; Published: 20 October 2017

Abstract: For theoretical designing of full-Heusler based spintroinc materials, people have long believed in the so-called Site Preference Rule (SPR). Very recently, according to the SPR, there are several studies on XA-type Hafnium-based Heusler alloys X_2YZ, i.e., Hf_2VAl, Hf_2CoZ (Z = Ga, In) and Hf_2CrZ (Z = Al, Ga, In). In this work, a series of Hf_2-based Heusler alloys, Hf_2VZ (Z = Al, Ga, In, Tl, Si, Ge, Sn, Pb), were selected as targets to study the site preferences of their atoms by first-principle calculations. It has been found that all of them are likely to exhibit the $L2_1$-type structure instead of the XA one. Furthermore, we reveal that the high values of spin-polarization of XA-type Hf_2VZ (Z = Al, Ga, In, Tl, Si, Ge, Sn, Pb) alloys have dropped dramatically when they form the $L2_1$-type structure. Also, we prove that the electronic, magnetic, and physics nature of these alloys are quite different, depending on the $L2_1$-type or XA-type structures.

Keywords: site preference; Hf-based full-Heusler compounds; first-principles study; band structures; magnetic properties; mechanical properties

1. Introduction

Heusler alloys are a noticeable class of intermetallic materials that represent as usual by the formula X_2YZ (often called full-Heusler) [1–15] or XYZ (usually named as half-Heusler) [16], where X, Y are transition-metal-element atoms and Z is a main group element. The structure of full-Heusler alloys consists of four interpenetrating fcc lattices with four equidistant sites as basis along the diagonal of the unit cell. According to the well-known Site Preference Rule (SPR) [1–15], when the valence of the X is larger than that of Y, the atomic sequence is X^A-Y^B-X^C-Z^D and the structure is the well-known $L2_1$ one with prototype Cu_2MnAl. Otherwise, the alloys crystallize in the so-called XA structure, where the sequence of the atoms is then X^A-X^B-Y^C-Z^D and the prototype is Hg_2CuTi. The latter alloys are also named as inverse Heusler alloys.

To the best of our knowledge, SPR has been applied extensively in the theoretical design of full-Heusler alloys and in predictions of their electronic, magnetic, and transport behavior. Some XA-type full-Heusler alloys, Mn_2CoAl [16], Ti_2MnAl [17], and Ti_2CoSi [18], were predicted to be novel spin-gapless semiconductors (SGSs) [19,20]. Furthermore, lots of XA-type full-Heusler alloys, Sc_2-, V_2-, Cr_2-, Mn_2-, Ti_2-, Zr_2-, and even Hf_2-based alloys, were revealed to be excellent half-metallic materials (HMMs) [21]. Surprisingly, one counterexample after another, including X_2CuAl [22] and Ti_2FeZ (Z = Al, Ga) alloys [6], has been reported very recently, in which these alloys show the $L2_1$-type structure and disobey the SPR, so that Y with more electrons enters the B sites.

In this work, a systematic theoretical work has been carried out to examine whether the conventional SPR was suitable for the Hf_2-based highly-ordered full-Heusler alloys. To this end, the competition between the XA and $L2_1$ orderings of Hf_2VZ (Z = Al, Ga, In, Tl, Si, Ge, Sn, Pb) full-Heusler alloys has been studied through the first-principles calculations. Our current work shows that not all the full-Heusler alloys obey the SPR, and further, the SPR can not be considered as a concise judgement principle for the structure of highly-ordered full-Heusler alloys. Remarkably, we exhibit that atomic site occupation in these Hf_2VZ alloys is decisive in determining their electronic, magnetic, and Slater-Pauling properties. For the $L2_1$-type Hf_2VZ (Z = Al, Ga, In, Tl, Si, Ge, Sn, Pb) full-Heusler alloys, the phase stability from the aspect of the formation energy and mechanical behaviors has also been examined in term of theory. Details of the results are shown in the following discussion.

2. Computational Details

First-principles electronic-structure calculations were performed using density function theory (DFT) implemented in the CASTEP code [23,24] according to the plane-wave pseudo-potential method. The generalized gradient approximation (GGA) [25] was adopted for the exchange-correlation functional. For the XA-type and $L2_1$-type Heusler alloys Hf_2VZ (Z = Al, Ga, In, Tl, Si, Ge, Sn, Pb), a Monkhorst-Pack special k-point mesh of $9 \times 9 \times 9$ was used in the Brillouin zone integrations with a cutoff energy of 400 eV and a self-consistent field tolerance of 10^{-6} eV. The quality of the k-point separation for the band structure calculation is 0.01 $Å^{-1}$.

As shown in Figure 1, the crystal structures of XA and $L2_1$ types Hf_2VZ Heusler alloys have been given. For the former, the two Hf atoms sitting at the two inequivalent sites, and Hf 1, Hf 2, V and Z atoms occupy the Wyckoff coordinates A (0, 0, 0), B (0.25, 0.25, 0.25), C (0.5, 0.5, 0.5) and D (0.75, 0.75, 0.75), respectively; For the latter, the two Hf atoms are essentially equivalent, and they have the same atomic environment. Hf 1, Hf 2, V and Z atoms occupy the Wyckoff coordinates A (0, 0, 0), B (0.5, 0.5, 0.5), C (0.25, 0.25, 0.25) and D (0.75, 0.75, 0.75), respectively.

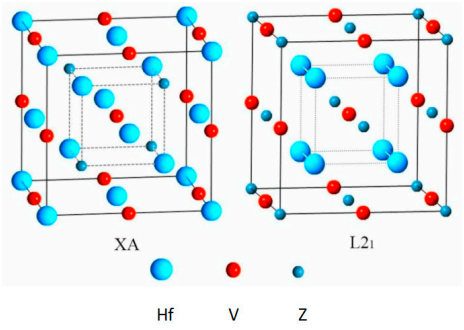

Figure 1. Crystal structures of XA and $L2_1$ types Hf_2VZ (Z = Al, Ga, In, Tl, Si, Ge, Sn, Pb) alloys. This $1 \times 1 \times 1$ super-cell system contains 16 atoms, i.e., $8 \times$ Hf, $4 \times$ V and $4 \times$ Z.

3. Results and Discussion

3.1. Competition of $L2_1$ and XA Structure Ordering in Full-Heusler Hf_2VZ Alloys

First, to confirm the ground state of Hf_2VZ (Z = Al, Ga, In, Tl, Si, Ge, Sn, Pb) full-Heusler alloys, the geometry optimization has been performed by calculating the total energies as functions of the lattice constant (cell volume) [26]. In this work, three possible magnetic states, i.e., paramagnetic (PM), ferrimangetic (FiM), and antiferromagnetic (AFM) states are taken into account. The PM (or nonmagnetic) state means that the constituent atoms of Hf_2VZ have no spin polarization. The FiM state implies that the spin magnetic moments of Hf atoms align anti-parallel to those of the V atoms, and the total magnetic moment is not equal to zero, while the AFM state means the spin magnetic moments of Hf atoms align antiparallelly to those of the V atoms, and the total magnetic

moment is equal to zero. For our Hf_2VZ (Z = Al, Ga, In, Tl, Si, Ge, Sn, Pb) full-Heusler alloys, the FiM state is the most stable among three magnetic states.

As shown in Figure 2, the total energy as functions of lattice constants of full-Heusler Hf_2VZ (Z = Al, Ga, In, Tl, Si, Ge, Sn, Pb) alloys with two atomic occupation orderings, XA and $L2_1$, and with their most stable magnetic state, FiM, have been exhibited. Obviously, for all these alloys, the $L2_1$ state has lower energies than XA state. Therefore, Hf_2VZ alloys studied in current work prefer to form the $L2_1$-type structure as ground state with equilibrium lattice constant of 6.69 Å, 6.66 Å, 6.90 Å, 6.89 Å, 6.56 Å, 6.61 Å, 6.82 Å and 6.90 Å, respectively. The obtained equilibrium lattice constants of these alloys with XA-type and $L2_1$-type structures, respectively, and the energy differences between these two structures ($\Delta E = E_{XA}^{total} - E_{L2_1}^{total}$) for Hf_2VZ (Z = Al, Ga, In, Tl, Si, Ge, Sn, Pb) alloys are also listed in Table 1. A higher value of ΔE indicates the $L2_1$-type structure is more stable than XA-type. The highest positive value of 0.71 eV/cell appears in Hf_2VGa alloy, reflecting that the site preference of V for the B position is quite strong. Hence, compared to other Hf_2-based Heusler alloys, XA-type Hf_2VGa maybe more difficult to synthesize experimentally due to its largest ΔE.

We should point out here that, as we said in the part of Introduction, Hf_2VZ alloys or even all the Hf-based full Heusler alloys should exhibit XA-type Heusler structure on basis of the SPR. Surprisingly, in current work, our results break the traditional SPR. Also, the data in this work, together with the latest scientific findings in References [6,22,27,28], are sufficient to demonstrate that not all the full-Heusler alloys X_2YZ obey the well-known SPR, especially X are low-valent transition metals. Since the SPR can not be regarded as the only way to determine the competition of XA and $L2_1$ structural ordering in Heusler alloys, alloys with $L2_1$-type structure should also be taken into account in the previous works [1–3,7–11].

Table 1. The calculated energy difference ΔE, lattice constant a, total and atomic spin magnetic moments for Hf_2VZ alloys with $L2_1$ and XA structures, respectively.

Alloy	Structure	ΔE (eV/cell)	a (Å)	M_t (μ_B/f.u.)	$M_{Hf\,1}$ (μ_B)	$M_{Hf\,2}$ (μ_B)	M_V (μ_B)	M_Z (μ_B)	Stable Structure
Hf_2VAl	XA	0.64	6.71	2	−0.65	0.14	2.62	−0.12	$L2_1$
	$L2_1$		6.69	1.65	−0.21	−0.21	2.19	−0.11	
Hf_2VGa	XA	0.71	6.68	1.99	−0.59	0.15	2.55	−0.13	$L2_1$
	$L2_1$		6.66	1.68	−0.13	−0.13	2.06	−0.12	
Hf_2VIn	XA	0.39	6.88	2	−0.75	−0.01	2.88	−0.12	$L2_1$
	$L2_1$		6.90	1.70	−0.24	−0.24	2.31	−0.13	
Hf_2VTl	XA	0.32	6.92	1.98	−0.79	−0.1	3.0	−0.12	$L2_1$
	$L2_1$		6.89	1.61	−0.17	−0.17	2.06	−0.11	
Hf_2VSi	XA	0.63	6.57	1.02	−0.74	−0.25	2.08	−0.06	$L2_1$
	$L2_1$		6.56	0.24	−0.03	−0.03	0.31	−0.01	
Hf_2VGe	XA	0.58	6.64	1.03	−0.83	−0.34	2.26	−0.06	$L2_1$
	$L2_1$		6.61	0.2	−0.02	−0.02	0.26	−0.01	
Hf_2VSn	XA	0.18	6.85	1	−1.07	−0.51	2.64	−0.05	$L2_1$
	$L2_1$		6.82	0.49	−0.06	−0.06	0.63	−0.03	
Hf_2VPb	XA	0.11	6.94	1	−1.17	−0.63	2.87	−0.04	$L2_1$
	$L2_1$		6.90	0.32	−0.03	−0.03	0.41	−0.02	

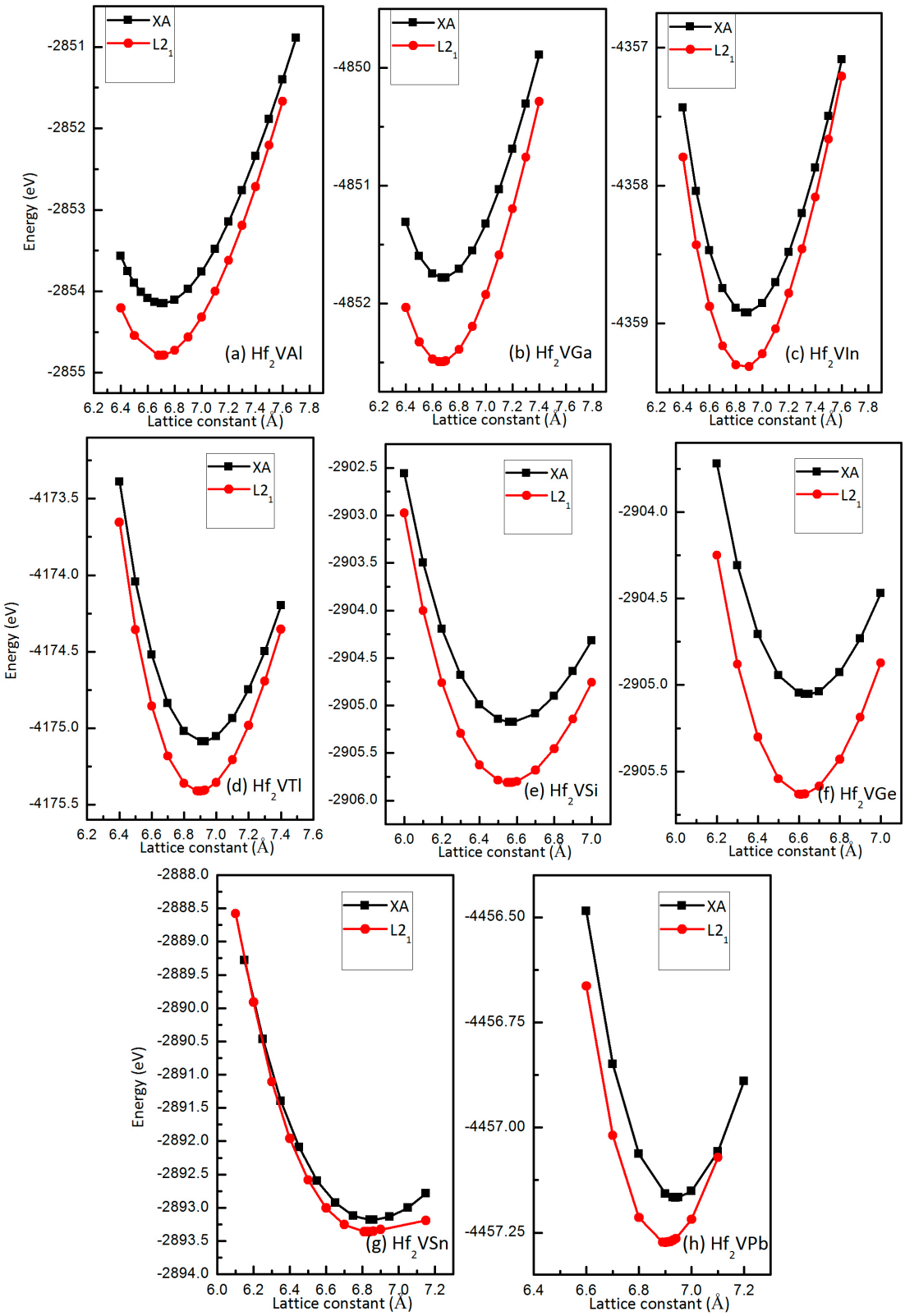

Figure 2. Calculated total energies of XA and $L2_1$ types Hf_2VAl (**a**); Hf_2VGa (**b**); Hf_2VIn (**c**); Hf_2VTl (**d**); Hf_2VSi (**e**); Hf_2VGe (**f**); Hf_2VSn (**g**); Hf_2VPb (**h**) alloys with respect to the lattice constant.

3.2. Structural and Mechanical Properties of Heusler-Based Hf_2VZ with $L2_1$-Type Ordering

Further, we aim to check the structural stability of the $L2_1$-type full-Heusler Hf_2VZ according to their calculated formation energies and mechanical properties. Similar methods [29,30] have been applied extensively to analyze the stability for Heusler alloys in term of theory. The formation energies of these alloys can be obtained from the following equation:

$$E_f = E^{total}_{Hf_2VZ} - (E^{bulk}_{Hf1} + E^{bulk}_{Hf2} + E^{bulk}_{V} + E^{bulk}_{Z}) \quad (1)$$

where $E^{total}_{Hf_2VZ}$ is the total energy of Hf_2VZ per formula unit, and E^{bulk}_{Hf1}, E^{bulk}_{Hf2}, E^{bulk}_{V}, and E^{bulk}_{Z} are the total energies per atom of each element in the bulk form for the Hf 1, Hf 2, V, and Z, respectively. The results have been given in Table 2, we can see that all these alloys have negative formation energies. Furthermore, the total energy of $L2_1$-type Hf_2VZ is lower than XA-type Hf_2VZ (see Figure 1), and thus, the E_f of $L2_1$-type Hf_2VZ should be lower than XA-type Hf_2VZ. This implies that $L2_1$-type Hf_2VZ should be more stable than the XA-type Hf_2VZ alloys.

Next, we come to the mechanical properties of these alloys and examine their stability based on achieved elastic constants C_{ij}. For these alloys with cubic structure, only three independent elastic constants (C_{11}, C_{12} and C_{44}) are needed to be taken into consideration, and the C_{ij} can be shown as below [31]:

$$\begin{pmatrix} C_{11} & C_{12} & C_{12} & 0 & 0 & 0 \\ C_{12} & C_{11} & C_{12} & 0 & 0 & 0 \\ C_{12} & C_{12} & C_{11} & 0 & 0 & 0 \\ 0 & 0 & 0 & C_{44} & 0 & 0 \\ 0 & 0 & 0 & 0 & C_{44} & 0 \\ 0 & 0 & 0 & 0 & 0 & C_{44} \end{pmatrix} \quad (2)$$

For a small strain on a cubic system, the change of elastic energy ΔE can be shown as below [32]:

$$\Delta E = \frac{V}{2} \sum_{i=1}^{6} \sum_{i=1}^{6} C_{ij} e_i e_j \quad (3)$$

where V stands for the volume of the unit cell. The strain tensors are always symmetric, and they can therefore be expressed more compactly as 6-component vectors, using the so-called Voigt notation. We select three strain tensors $(0,0,0,\delta,\delta,\delta)$, $(\delta,\delta,0,0,0,0)$ and $(\delta,\delta,\delta,0,0,0)$ to obtain the elastic constants:

$$\frac{\Delta E_1}{V} = \frac{3}{2} C_{44} \delta^2 \quad (4)$$

$$\frac{\Delta E_2}{V} = (C_{11} + C_{12}) \delta^2 \quad (5)$$

$$\frac{\Delta E_3}{V} = \frac{3}{2} (C_{11} + C_{12}) \delta^2 \quad (6)$$

where $\Delta E_1, \Delta E_2, \Delta E_3$ are the change of elastic energy for small strain tensors $(0,0,0,\delta,\delta,\delta)$, $(\delta,\delta,0,0,0,0)$ and $(\delta,\delta,\delta,0,0,0)$, respectively.

Based on obtained C_{ij}, the mechanical properties, including bulk modulus B, shear modulus G, Voigt's shear modulus G_V, Reuss's shear modulus G_R, Young's modulus E, Pugh's ratio B/G, anisotropy factor A, of Hf_2VZ can be calculated by using the following equations [29]:

$$B = \frac{C_{11} + 2C_{12}}{3} \quad (7)$$

$$G = \frac{G_R + G_V}{2} \quad (8)$$

$$G_V = \frac{C_{11} - C_{12} + 3C_{44}}{5} \tag{9}$$

$$G_R = \frac{5(C_{11} - C_{12})C_{44}}{4C_{44} + 3(C_{11} - C_{12})} \tag{10}$$

$$E = \frac{9GB}{3B + G} \tag{11}$$

$$A = \frac{2C_{44}}{C_{11} - C_{12}} \tag{12}$$

As shown in Table 2, we can see that all these alloys with $L2_1$-type structure are mechanical stable due to their calculated elastic constants follow the generalized elastic stability criteria [33]:

$$C_{44} > 0 \tag{13}$$

$$\frac{(C_{11} - C_{12})}{2} > 0 \tag{14}$$

$$B > 0 \tag{15}$$

$$C_{12} < B < C_{11} \tag{16}$$

Moreover, some special mechanical properties of these alloys can also be observed from Table 2. We addressed some as follows: (1) the values of B/G of these alloys are all larger than 1.75, reflecting they are ductile according to Pugh's criteria; (2) the values of A for all these alloys are not equal to 1, meaning the fact that they are anisotropic; (3) as is known, the higher the value of E, the stiffer is the materials, and therefore, the relative stiffer order of these Hf_2VZ materials is Hf_2VAl > Hf_2VSi > Hf_2VGa > Hf_2VGe > Hf_2VIn > Hf_2VSn > Hf_2VTl > Hf_2VPb.

Table 2. Calculated elastic constants C_{ij}, bulk modulus B, shear modulus G, Young's modulus E (GPa), Pugh's ratio B/G, anisotropy factor A, and formation energy (eV) for Hf_2VZ alloys with $L2_1$ structure.

Alloy	C_{11}	C_{12}	C_{44}	B	G	E	B/G	Formation Energy	Anisotropy Factor
Hf_2VAl	164.4	117.6	73.0	133.2	46.8	124.6	2.8	−0.54	3.10
Hf_2VGa	143	104.3	72.9	117.9	43.0	115.10	2.7	−1.19	3.76
Hf_2VIn	179.8	154.3	49.7	162.8	28.9	82.0	5.6	−0.05	3.89
Hf_2VTl	110.4	100.1	46.8	103.5	20.5	57.9	5.0	−0.85	9.08
Hf_2VSi	191	146.9	63.7	161.6	41.6	115.12	3.8	−0.66	2.88
Hf_2VGe	158.2	123.1	54.1	134.8	34.5	95.4	3.9	−0.41	3.08
Hf_2VSn	187.5	155.6	42.2	166.2	28.5	81.1	5.8	−0.07	2.64
Hf_2VPb	109.1	97.9	18.2	101.6	11.4	32.9	8.9	−0.91	3.25

3.3. Calculated Electronic Behaviors of $L2_1$ and XA Types Hf_2VZ

Electronic-structure calculation theory has clearly indicated [20,34,35] that the spintonic properties of materials among Heusler family has an unusual sensibility to the atomic occupation in crystal cell. Hence, in this section, a discussion about the spintronic property differences, including the magnetic, electronic, half-metallic, and the spin polarization ratio (p), between the XA and $L2_1$ Hf_2VZ (Z = Al, Ga, In, Tl, Si, Ge, Sn, Pb) full-Heusler alloys should be performed. Figures 3–5 show the calculated band structures for XA and $L2_1$ types Hf_2VZ (Z = Al, Ga, In, Tl, Si, Ge, Sn, Pb) at their equilibrium lattice constants.

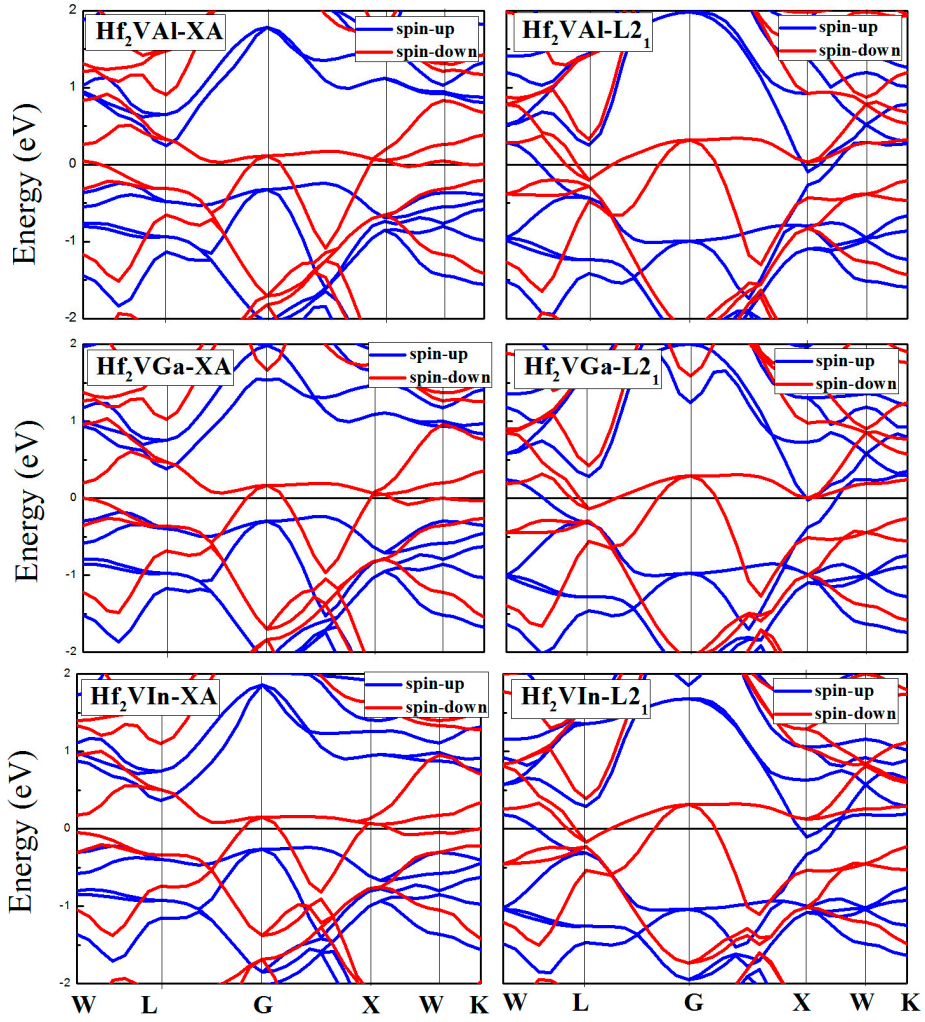

Figure 3. Calculated band structures of XA and $L2_1$ types Hf_2VZ (Z = Al, Ga, In) alloys.

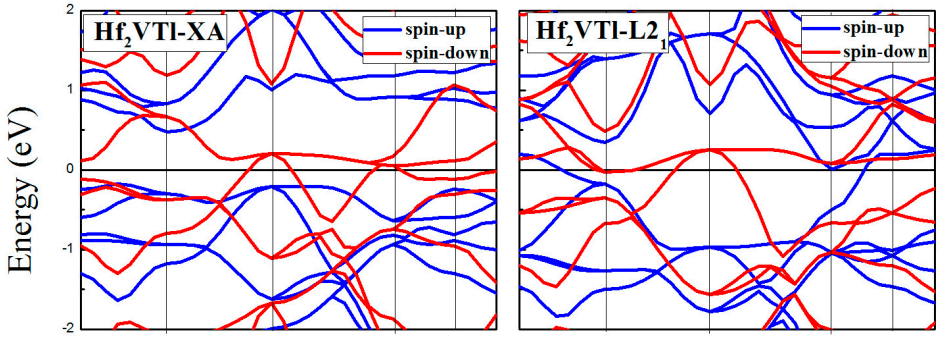

Figure 4. *Cont.*

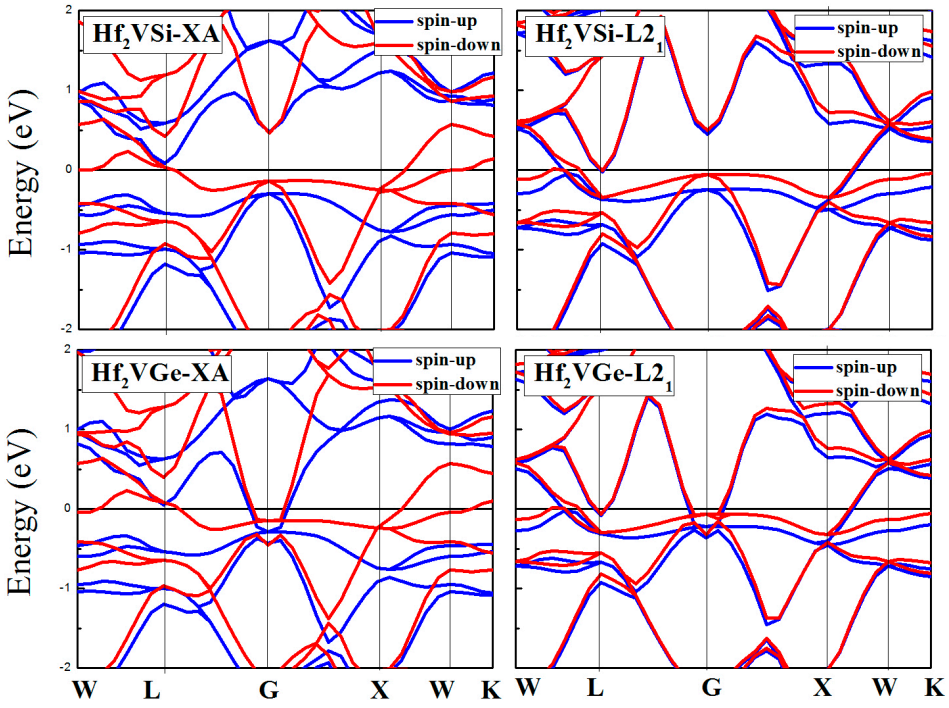

Figure 4. Calculated band structures of XA and $L2_1$ types Hf_2VZ (Z = Tl, Si, Ge) alloys.

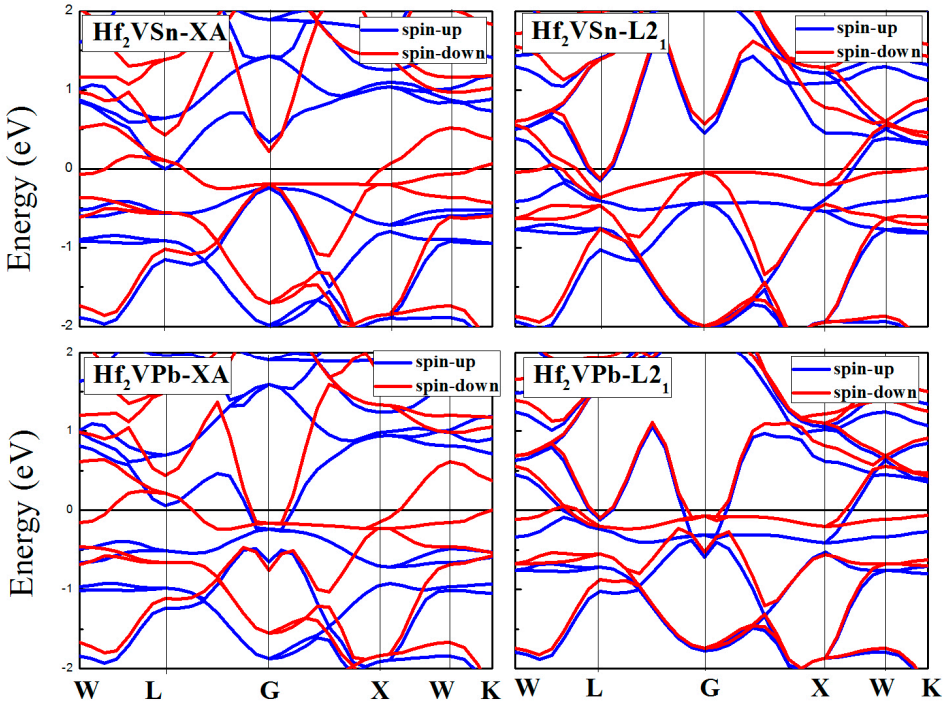

Figure 5. Calculated band structures of XA and $L2_1$ types Hf_2VZ (Z = Sn and Pb) alloys.

For XA atomic ordering, Hf_2VZ (Z = Al, Ga, In, Tl, Si, Sn) alloys are excellent half-metallic materials since there is a semiconducting-type band gap in the spin-up direction and the Fermi level locates between the opened gap. However, in the spin-down direction, the semiconducting-type band gap disappeared: although an opened gap can be observed near the Fermi level, the Fermi level has overlapped with the spin-down bands in varying degrees. In the spin-up channel, the significant factors, including the

calculated valence band maximum (VBM), conduction band minimum (CBM), semiconducting band gap, and spin-flip/half-metallic gap, have been given in Table 3, the semiconducting band gap [36] is the sum of the absolute values of CBM and VBM, and the spin-flip/half-metallic gap [36] is defined as the minimum value of the two absolute values of CBM and VBM. The semiconducting band gap values of these alloys are 0.46 eV for Hf_2VAl, 0.59 eV for Hf_2VGa, 0.59 eV for Hf_2VIn, 0.64 eV for Hf_2VTl, 0.35 eV for Hf_2VSi, 0.30 eV for Hf_2VSn, respectively. The spin-flip/half-metallic gap values of these alloys are 0.23 eV for Hf_2VAl, 0.23 eV for Hf_2VGa, 0.22 eV for Hf_2VIn, 0.17 eV for Hf_2VTl, 0.07 eV for Hf_2VSi, 0.04 eV for Hf_2VSn, respectively. For XA atom ordering Hf_2VGe and Hf_2VPb alloys, semiconducting band gaps in the both directions disappeared and both alloys exhibit common metallic properties.

Table 3. Calculated valence band maximum (VBM), conduction band minimum (CBM), semiconducting band gaps, spin-flip gap/half-metallic gaps and spin polarization ratio (p) of Hf_2VZ alloys with $L2_1$ and XA structures, respectively.

Alloy	Structure	CBM	VBM	Band Gap	Half-Metallic Gap	p (%)
Hf_2VAl	XA	0.23	−0.23	0.46	0.23	100
	$L2_1$	-	-	-	-	48
Hf_2VGa	XA	0.36	−0.23	0.59	0.23	100
	$L2_1$	-	-	-	-	52
Hf_2VIn	XA	0.37	−0.22	0.59	0.22	100
	$L2_1$	-	-	-	-	36
Hf_2VTl	XA	0.47	−0.17	0.64	0.17	100
	$L2_1$	-	-	-	-	40
Hf_2VSi	XA	0.07	−0.28	0.35	0.07	100
	$L2_1$	-	-	-	-	39
Hf_2VGe	XA	-	-	-	-	88
	$L2_1$	-	-	-	-	33
Hf_2VSn	XA	0.04	−0.26	0.30	0.04	100
	$L2_1$	-	-	-	-	56
Hf_2VPb	XA	-	-	-	-	94
	$L2_1$	-	-	-	-	36

For Hf_2VZ (Z = Al, Ga, In, Tl, Si, Sn) alloys with the XA structure, the V and Hf atoms occupy sites with same symmetry in XA-type Heusler structure, and the hybridization of their d orbitals creates 5 bonding bands ($3t_{2g}$ and $2e_g$) and 5 non-bonding bands ($2e_u$ and $3t_{1u}$). Then, the 5 V-Hf bonding d hybrids hybridize in turn with d orbitals of Hf, again forming bonding and anti-bonding bands, while the 5 non-bonding bands ($2e_u$ and $3t_{1u}$) still exist with no hybridizing. Finally, the distribution of the 15 d orbitals in the minority-spin direction can be determined, i.e., $3t_{2g}$, $2e_g$, $2e_u$, $3t_{1u}$, $3t_{2g}$, and $2e_g$, from the high-energy level to the low-energy level. Also, we cannot ignore that Z creates 1s and 3p bands which are totally occupied in Hf_2VZ and are also below the above-mentioned 15 d orbitals. Therefore, their semiconducting-type band gaps are created by the separated Γ_{15} and Γ_{25} states, coming from the bonding t_{2g} and antibonding t_{1u} states.

The calculated total and partial density of states (TDOS and PDOS) for the six Hf_2VZ (Z = Al, Ga, In, Tl, Si, Sn) alloys with XA and $L2_1$ atomic orderings and for equilibrium lattice constants have also been calculated in this work to deepen the understanding of their electronic properties. As an example, the results of Hf_2VAl and Hf_2VSi alloys are given in Figure 6. Clearly, from the figure, a semiconducting band gap can be found in spin-up direction for XA-type Hf_2VZ (Z = Al, Ga, In, Tl, Si, Sn) alloys, which is in a good agreement with above-mentioned band structures.

The DOS can be widely used to analyze the bonding/anti-bonding states and the gap formation and similar analytical approach can be observed in References [19,29]. In the spin-up channel, the main peaks of Hf 2 and V atoms occurred at around −0.5 eV. In the spin-down channel, in the similar

energy region (around −0.5 eV), for V and Hf 2 atoms, such hybridized peaks appeared at the same time. Therefore, the hybridization between the V and Hf 2 atoms that formed strong bonding states at around −0.5 eV. Above the Fermi level, in the spin-up channel, the anti-bonding peak can be found at around 1 eV mainly arise from the Hf 1-d electrons, and in the spin-down channel, no opposite energy states are observed. Moreover, in the spin-up channel, the corresponding bonding-antibonding states led to the formation of an opened band gap, and the Fermi level, exactly, locates between the gap.

For $L2_1$ type atomic ordering, the band structures and the DOS have a big difference with XA type atomic ordering. Namely, all the Hf_2VZ alloys investigated in this work show conventional metallic behaviors without semiconducting-type band gaps at Fermi level in both spin channels. As shown in Figures 3–6, both spin-up and spin-down bands are crossed by the Fermi level.

Moreover, from the obtained total DOS, we calculated the spin polarization (p) at Fermi energy of XA and $L2_1$ types Hf_2VZ. The spin polarization p (%) that can be defined as the ratio of the difference to sum of the DOS values of spin up and spin down version at the Fermi-level [13,16], represented by mathematical formulation as a percent;

$$p = \frac{n\uparrow\left(E_f\right) - n\downarrow\left(E_f\right)}{n\uparrow\left(E_f\right) + n\downarrow\left(E_f\right)} \times 100\% \quad (17)$$

where the $n\uparrow$ (E_f) and $n\downarrow$ (E_f) stand for the spin-dependent DOS around the Fermi level. The results have been given in Table 3, we can see that the p of XA-type Hf_2VZ are quite high (>88%), even some alloys (such as Hf_2VAl) have completely spin polarization (100%). High-spin-polarization materials are very useful in spintronic application. However, the $L2_1$-type Hf_2VZ exhibit pretty low spin polarization (<56%). This also implies that the novel spintronic properties (such as half-metallic properties) in XA type structure are disappeared as these alloys form $L2_1$ type structure.

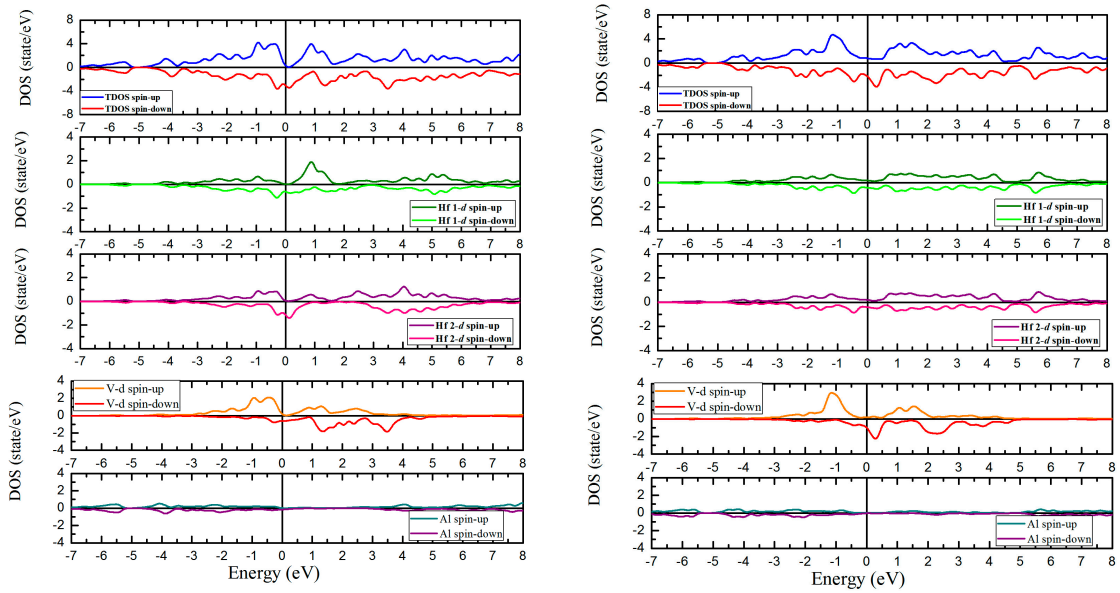

Figure 6. *Cont.*

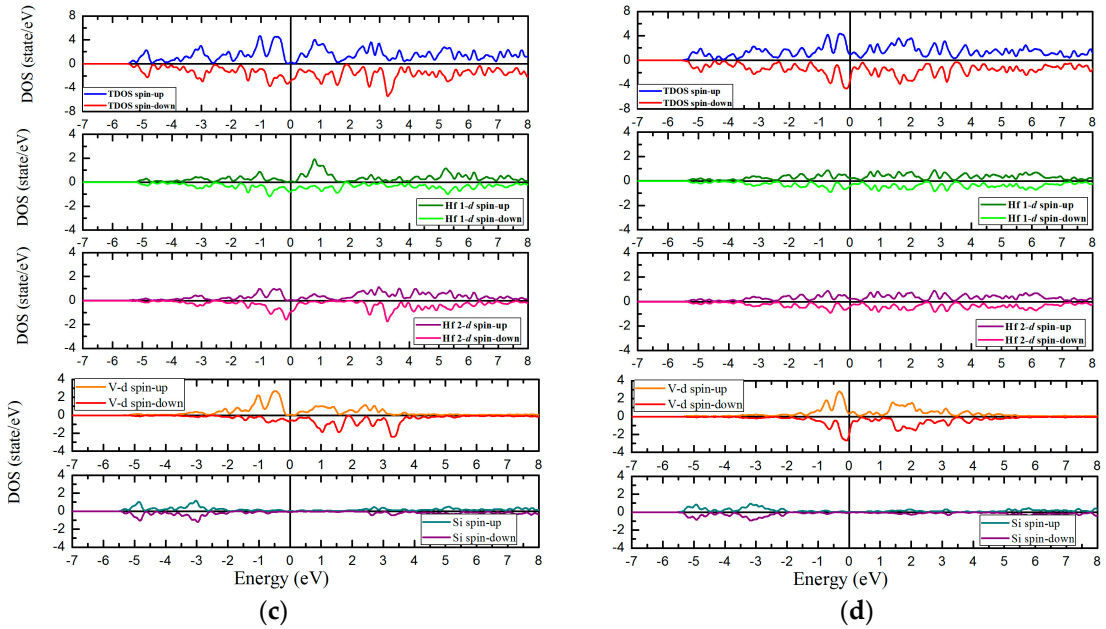

Figure 6. Calculated band structures of XA type Hf_2VAl (**a**); $L2_1$ type Hf_2VAl (**b**); XA type Hf_2VSi (**c**); $L2_1$ type Hf_2VSi (**d**); respectively.

3.4. Magnetic and Slater-Pauling Properties of $L2_1$ and XA Types Hf_2VZ

Finally, in this section, we come to discuss the magnetism and Slater-Pauling rule of $L2_1$ and XA types Hf_2VZ (Z = Al, Ga, In, Tl, Si, Ge, Sn, Pb) alloys. The total and atomic magnetic moments of these alloy with XA and $L2_1$ atomic ordering are shown in Table 1. Obviously, all these alloys, with either XA or $L2_1$ type structures, exhibit FiM properties with the atomic magnetic moments of Hf antiparalled aligned with that of V atoms. Based on Table 1, V carries the largest moment and therefore, V atom makes the most contribution to the total magnetic moment.

For XA-type Hf_2VZ full-Heusler materials, their total magnetic moments are almost integer values (2 μ_B/f.u. or 1 μ_B/f.u.), reflecting their high spin polarization properties. Furthermore, from Table 1, we can see that their total magnetic moments follow the well-known Slater-Pauling rule [37]:

$$M_t = Z_t - 18 \tag{18}$$

where the M_t stands for the total magnetic moment of these materials and the Z_t means the number of total of valence electrons in Hf_2VZ alloys. For $L2_1$ type Hf_2VZ full-Heusler materials, their total magnetic moments are all largely deviated from integer values, indicating the half-metallic properties have been totally destroyed when these alloys are in $L2_1$ type structure. For Hf_2VSi and Hf_2VGe, both alloys have a very weak moment of 0.24 μ_B/f.u. and 0.20 μ_B/f.u., respectively. Therefore, the $L2_1$ type Hf_2VZ full-Heusler alloys do not obey the above-mentioned Slater-Pauling rule.

The magnetism for XA and $L2_1$ types full-Heusler alloys Hf_2VZ (Z = Al, Ga, In, Tl, Si, Sn) alloys at their strained lattice constants has also been examined. As an example, the results of Hf_2VAl and Hf_2VGa have been given in Figure 7. According to the Slater-Pauling and generalized electron-filling rules [11,13], the integer values of total magnetic moments which follow the Slater-Pauling rule indicate the half-metallic properties of materials and thus stand for their high spin polarization. From Figure 7, we can see that the high spin polarization properties of XA type Hf_2VZ (Z = Al, Ga, In, Tl, Si, Sn) alloys are very robust, however, the region with high spin polarization (integer values of total magnetic moments) of $L2_1$-type Hf_2VZ alloys is extraordinarily narrow. For the atomic magnetic moments of XA and $L2_1$ types Hf_2VZ, the values of Hf decreases, whereas the V atom, it increases.

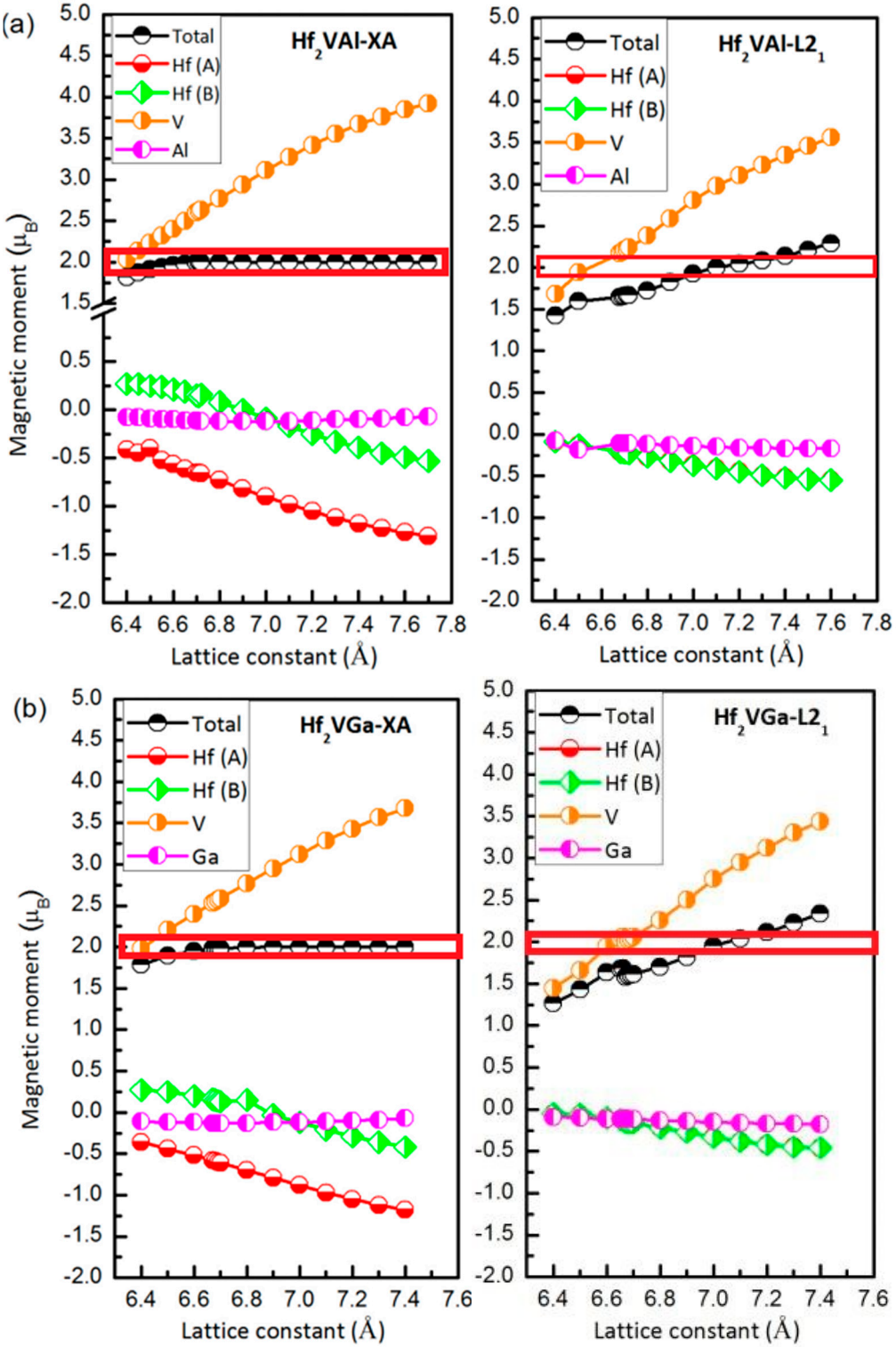

Figure 7. (**a**,**b**) Calculated total and atomic spin magnetic moments of Hf_2VZ (Z = Al, Ga) alloys as functions of the lattice constant. The red boxes show the high-spin polarization regions.

4. Conclusions

To sum up, the atomic occupation of a series of Hf_2-based full-Heusler alloys was investigated by theoretical first-principle calculations. We observed that all Hf_2V-based alloys studied in current work are likely to form the $L2_1$ structure instead of XA structure. Our results also indicate that the spintronic

properties (half-metallic or high spin-polarization properties), and Slater-Pauling behaviors that exist in XA for Hf_2VZ are fully destroyed in $L2_1$. With our study, it is clear that not all full-Heusler alloys X_2YZ obey the SPR, especially when X are low valence metal elements.

Acknowledgments: Funding for this research was proved by National Key R&D Program of China 2017YFA0206303, and National Natural Science Foundation of China, Grant No. 11574374.

Author Contributions: Zhenxiang Cheng conceived and designed the project; Xiaotian Wang performed the calculations and prepared this manuscript; Xiaotian Wang analyzed the data; Wenhong Wang and Zhenxiang Cheng discussed the results.

Conflicts of Interest: The authors declare no conflict of interest.

References

1. Hu, Y.; Zhang, J.M. The structural, electronic, magnetic, elastic properties of new Heusler alloys Hf_2CrZ (Z = Al, Ga, In): A first-principles study. *Solid State Commun.* **2017**, *259*, 1–6. [CrossRef]
2. Zhang, L.; Gao, Y.C. Electronic structures, magnetic properties and half-metallicity in the heusler alloy Hf_2VAl. *Chin. J. Phys.* **2017**, *55*, 1466–1472. [CrossRef]
3. Hu, Y.; Zhang, J.M. First-principles study of the Hf-based Heusler alloys: Hf_2CoGa and Hf_2CoIn. *J. Magn. Magn. Mater.* **2017**, *421*, 1–6. [CrossRef]
4. Dahmane, F.; Mogulkoc, Y.; Doumi, B.; Tadjer, A.; Khenata, R.; Omran, S.B.; Rai, D.P.; Murtaza, G.; Varshney, D. Structural, electronic and magnetic properties of Fe_2-based full Heusler alloys: A first principle study. *J. Magn. Magn. Mater.* **2016**, *407*, 167–174. [CrossRef]
5. Bayar, E.; Kervan, N.; Kervan, S. Half-metallic ferrimagnetism in the Ti_2CoAl Heusler compound. *J. Magn. Magn. Mater.* **2011**, *323*, 2945–2948. [CrossRef]
6. Zhang, X.J.; Liu, Z.H.; Zhang, Y.J.; Liu, H.Y.; Liu, G.D.; Cui, Y.T.; Ma, X.Q. Theoretical and experimental study of the phase formation for Ti_2YAl and $Ti_2Y'Ga$ (Y = Co, Fe; Y′ = Cr, Fe). *Intermetallics* **2016**, *73*, 26–30. [CrossRef]
7. Wang, X.T.; Lin, T.T.; Rozale, H.; Dai, X.F.; Liu, G.D. Robust half-metallic properties in inverse heusler alloys composed of 4d transition metal elements: Zr_2RhZ (Z = Al, Ga, In). *J. Magn. Magn. Mater.* **2016**, *402*, 190–195. [CrossRef]
8. Deng, Z.Y.; Zhang, J.M. Half-metallic and magnetic properties of full-heusler alloys Zr_2CrZ (Z = Ga, In) with Hg_2CuTi-type structure: A first-principles study. *J. Magn. Magn. Mater.* **2016**, *397*, 120–124. [CrossRef]
9. Fang, Q.L.; Zhang, J.M.; Xu, K.W. Magnetic properties and origin of the half-metallicity of Ti_2MnZ (Z = Al, Ga, In, Si, Ge, Sn) Heusler alloys with the Hg_2CuTi-type structure. *J. Magn. Magn. Mater.* **2014**, *349*, 104–108. [CrossRef]
10. Li, J.; Zhang, Z.; Lu, Z.; Xie, H.; Fang, W.; Li, S.; Liang, C.; Yin, F. The strain induced band gap modulation from narrow gap semiconductor to half-metal on Ti_2CrGe: A first principles study. *AIP Adv.* **2015**, *5*, 156404. [CrossRef]
11. Skaftouros, S.; Ozdogan, K.; Sasioglu, E.; Galanakis, I. Generalized Slater-Pauling rule for the inverse Heusler compounds. *Phys. Rev. B* **2013**, *87*, 4469–4487. [CrossRef]
12. Skaftouros, S.; Ozdogan, K.; Sasıoglu, E.; Galanakis, I. Search for spin gapless semiconductors: The case of inverse Heusler compounds. *Appl. Phys. Lett.* **2013**, *102*, 022402. [CrossRef]
13. Zhang, X.M.; Xu, G.Z.; Du, Y.; Liu, E.K.; Liu, Z.Y.; Liu, G.D.; Wang, W.H.; Wu, G.H. Phase stability, magnetism and generalized electron-filling rule of vanadium-based inverse Heusler compounds. *EPL* **2013**, *104*, 27012. [CrossRef]
14. Jakobsson, A.; Mavropoulos, P.; Sasioglu, E.; Blugel, S.; Lezaic, M.; Sanyal, B.; Galanakis, I. First-principles calculations of exchange interactions, spin waves, and temperature dependence of magnetization in inverse-Heusler-based spin gapless semiconductors. *Phys. Rev. B* **2015**, *91*, 2445–2447. [CrossRef]
15. Li, J.; Jin, Y. Half-metallicity of the inverse heusler alloy Mn_2CoAl (001) surface: A first-principles study. *Appl. Surf. Sci.* **2013**, *283*, 876–880. [CrossRef]
16. Wang, X.T.; Cheng, Z.X.; Liu, G.D. Largest magnetic moments in the half-Heusler alloys XCrZ (X = Li, K, Rb, Cs; Z = S, Se, Te): A first-principles study. *Materials* **2017**, *10*, 1078. [CrossRef] [PubMed]

17. Galanakis, I.; Ozdogan, K.; Sasioglu, E.; Blugel, S. Conditions for spin-gapless semiconducting behavior in Mn_2CoAl inverse heusler compound. *J. Appl. Phys.* **2014**, *115*, 668. [CrossRef]
18. Feng, W.; Fu, X.; Wan, C.; Yuan, Z.; Han, X.; Quang, N.V.; Cho, S. Spin gapless semiconductor like Ti_2MnAl film as a new candidate for spintronics application. *Phys. Status Solidi RRL Rapid Res. Lett.* **2016**, *9*, 641–645. [CrossRef]
19. Birsan, A.; Palade, P.; Kuncser, V. Prediction of half metallic properties in Ti_2CoSi Heusler alloy based on density functional theory. *J. Magn. Magn. Mater.* **2013**, *331*, 109–112. [CrossRef]
20. Bainsla, L.; Mallick, A.I.; Raja, M.M.; Coelho, A.A.; Nigam, A.K.; Johnson, D.D.; Alam, A.; Suresh, K.G. Origin of spin gapless semiconductor behavior in CoFeCrGa: Theory and experiment. *Phys. Rev. B Condens. Matter.* **2015**, *92*, 45201. [CrossRef]
21. Groot, R.A.D.; Mueller, F.M.; Engen, P.G.V.; Buschow, K.H.J. New class of materials: Half-metallic ferromagnets. *Phys. Rev. Lett.* **1983**, *50*, 2024–2027. [CrossRef]
22. Luo, H.; Xin, Y.; Liu, B.; Meng, F.; Liu, H.; Liu, E.; Wu, G. Competition of $L2_1$, and XA structural ordering in heusler alloys X_2CuAl (X = Sc, Ti, V, Cr, Mn, Fe, Co, Ni). *J. Alloys Compd.* **2016**, *665*, 180–185. [CrossRef]
23. Payne, M.C.; Teter, M.P.; Allan, D.C.; Arias, T.A.; Joannopoulos, J.D. Iterative minimization techniques for ab initio total-energy calculations: Molecular dynamics and conjugate gradients. *Rev. Mod. Phys.* **1992**, *64*, 1045. [CrossRef]
24. Segall, M.D.; Lindan, P.J.; Probert, M.A.; Pickard, C.J.; Hasnip, P.J.; Clark, S.J.; Payne, M.C. First-principles simulation: Ideas, illustrations and the CASTEP code. *J. Phys. Condens. Matter* **2002**, *14*, 2717–2744. [CrossRef]
25. Perdew, J.P.; Burke, K.; Ernzerhof, M. Generalized gradient approximation made simple. *Phys. Rev. Lett.* **1996**, *77*, 3865–3868. [CrossRef] [PubMed]
26. Qin, G.; Wu, W.; Hu, S.; Tao, Y.; Yan, X.; Jing, C.; Li, X.; Gu, H.; Cao, S.; Ren, W. Effect of swap disorder on the physical properties of the quaternary heusler alloy PdMnTiAl: A first-principles study. *IUCrJ* **2017**, *4*, 506–511. [CrossRef] [PubMed]
27. Galehgirian, S.; Ahmadian, F. First principles study on half-metallic properties of heusler compounds Ti_2VZ (Z = Al, Ga, and In). *Solid State Commun.* **2015**, *202*, 52–57. [CrossRef]
28. Lukashev, P.; Kharel, P.; Gilbert, S.; Staten, B.; Hurley, N.; Fuglsby, R.; Huh, Y.; Valloppilly, S.; Zhang, W.; Yang, K.; et al. Investigation of spin-gapless semiconductivity and half-metallicity in Ti_2MnAl-based compounds. *Appl. Phys. Lett.* **2016**, *108*, 156404. [CrossRef]
29. Wang, X.; Cheng, Z.; Wang, J.; Liu, G. A full spectrum of spintronic properties demonstrated by a $C1_b$-type Heusler compound Mn_2Sn subjected to strain engineering. *J. Mater. Chem. C* **2016**, *4*, 8535–8544. [CrossRef]
30. Benkaddour, K.; Chahed, A.; Amar, A.; Rozale, H.; Lakdja, A.; Benhelal, O.; Sayede, A. First-principles study of structural, elastic, thermodynamic, electronic and magnetic properties for the quaternary Heusler alloys CoRuFeZ (Z = Si, Ge, Sn). *J. Alloys Compd.* **2016**, *687*, 211–220. [CrossRef]
31. Gooch, J.W. *Elastic Constant*; Springer: New York, NY, USA, 2011.
32. Zhao, J.S.; Gao, Q.; Li, L.; Xie, H.H.; Hu, X.R.; Xu, C.L.; Deng, J.-B. First-principles study of the structure, electronic, magnetic and elastic properties of half-Heusler compounds LiXGe (X = Ca, Sr and Ba). *Intermetallics* **2017**, *89*, 65–73. [CrossRef]
33. Born, M.; Huang, K. *Dynamical Theory of Crystal Lattices*; Clarendon Press: Oxford, UK, 1954.
34. Wang, X.T.; Cheng, Z.X.; Wang, J.L.; Rozale, H.; Wang, L.Y.; Yu, Z.Y.; Liu, G.D. Strain-induced diverse transitions in physical nature in the newly designed inverse Heusler alloy Zr_2MnAl. *J. Alloys Compd.* **2016**, *686*, 549–555. [CrossRef]
35. Wang, X.; Cheng, Z.; Khenata, R.; Wu, Y.; Wang, L.; Liu, G. Lattice constant changes leading to significant changes of the spin-gapless features and physical nature in a inverse heusler compound Zr_2MnGa. *J. Magn. Magn. Mater.* **2017**, *444*, 313–318. [CrossRef]

36. Ahmadian, F. Half-metallic ferromagnetism in the Ti_2FeGe Heusler compound: A first-principles study. *J. Supercond. Nov. Magn.* **2013**, *26*, 381–388. [CrossRef]
37. Galanakis, I.; Dederichs, P.H.; Papanikolaou, N. Slater-Pauling behavior and origin of the half-metallicity of the full-Heusler alloys. *Phys. Rev. B* **2002**, *66*, 553–562. [CrossRef]